NANO · MICRO small
www.small-journal.com

Anomalous Colloidal Motion under Strong Confinement

*Irene Abelenda-Núñez, Francisco Ortega, Ramón G. Rubio, and Eduardo Guzmán**

Diffusion of biological macromolecules in the cytoplasm is a paradigm of colloidal diffusion in an environment characterized by a strong restriction of the accessible volume. This makes of the understanding of the physical rules governing colloidal diffusion under conditions mimicking the reduction in accessible volume occurring in the cell cytoplasm, a problem of a paramount importance. This work aims to study how the thermal motion of spherical colloidal beads in the inner cavity of giant unilamellar vesicles (GUVs) is modified by strong confinement conditions, and the viscoelastic character of the medium. Using single particle tracking, it is found that both the confinement and the environmental viscoelasticity lead to the emergence of anomalous motion pathways for colloidal microbeads encapsulated in the aqueous inner cavity of GUVs. This anomalous diffusion is strongly dependent on the ratio between the volume of the colloidal particle and that of the GUV under consideration as well as on the viscosity of the particle's liquid environment. Therefore, the results evidence that the reduction of the free volume accessible to colloidal motion pushes the diffusion far from a standard Brownian pathway as a result of the change in the hydrodynamic boundary conditions driving the particle motion.

1. Introduction

The complexity in cells arises in part from the existence of various biochemical and biophysical processes that take place in the cytoplasm, which is an environment characterized by a sharp reduction in the free volume accessible for the diffusion of biological macromolecules and supramolecular objects. This is the result of the combination of two different factors: i) Confinement (or caging), and ii) crowding.[1,2] The former is associated with the presence of the plasma membrane, which prevents leakage of the cytoplasmic content and provides mechanisms for the entry of nutrients and other compounds into the cellular interior and the expulsion of residues. Therefore, the plasma membrane should be considered as a fixed boundary which limits the volume accessible to macromolecular diffusion. On the other hand, crowding is caused by the high density of organelles, supramolecular structures (cytoskeletal filaments) and biological macromolecules (proteins, polysaccharides, and nucleic acids), which account for 40% of the total volume contained in the cytoplasm.[3–5] The volume exclusion associated with the complexity of the cytoplasm leads to non-specific steric repulsion, depletion attraction, and reduced translational degrees of freedom between macromolecules, resulting in a deviation of the transport phenomena from a standard Brownian diffusion pathway.[6–10] This has implications for various biochemical and biophysical functions of living cells,[11,12] for example, modify stability, aggregation and conformation of proteins, alter the rate of enzymatic catalysis, modulate intermolecular interactions, drive anomalous diffusion of macromolecules or induce phase separation or microcompartmentalization.[2,13–18] The above effect enables the cytoplasm to be defined as a glassy, non-ergodic, viscous emulsion of coexisting fluids.[19] Despite the importance of the crowding and confinement in the dynamic processes involving biological macromolecules in cells, most of what is currently known about their effects is focused on experiments performed under solution conditions using inert synthetic macromolecular agents, such as Ficoll 70, poly(ethylene oxide) or dextran.[1] It should be emphasized that motion under a strong reduction of the accessible region is not limited to the biological field, and can also be found in situations of industrial interest, for example, the diffusion of particles confined in nanocomposites and gels or different separation methods.[20–24]

The use of artificial lipid vesicles as models appears to be a promising alternative for understanding some fundamental various of different physical processes occurring within cellular systems. The embedding of synthetic inert agents that impart a viscoelastic character to the fluid encapsulated in the internal cavity of giant unilamellar vesicles (GUVs) has contributed to the understanding of how the confinement and the viscoelasticity of the medium contribute the optimization of the kinetic and equilibrium aspects of biochemical processes,[10,25,26]

I. Abelenda-Núñez, F. Ortega, R. G. Rubio, E. Guzmán
Departamento de Química Física
Facultad de Ciencias Químicas
Universidad Complutense de Madrid
Ciudad Universitaria s/n.
Madrid 28040, Spain
E-mail: eduardogs@quim.ucm.es
F. Ortega, E. Guzmán
Unidad de Materia Condensada, Instituto Pluridisciplinar
Universidad Complutense de Madrid
Paseo Juan XXIII 1., Madrid 28040, Spain
The ORCID identification number(s) for the author(s) of this article can be found under https://doi.org/10.1002/smll.202302115.

DOI: 10.1002/smll.202302115

although this type of model is far from what can result from the complexity of a cell. Nevertheless, they offer a good opportunity to modulate the exclusion of volume almost at will by controlling the dimension of the GUVs (cage size) and the viscosity of the fluid contained in its inner cavity.[26,27] Furthermore, the use of GUVs also provides a good opportunity to control the potential effect of the chemical nature of the container wall on the balance of interactions affecting the motion of biological macromolecules within the aqueous environment. This is important because it has recently been found that a preferential volume exclusion near the membrane can alter the balance of interactions and hence the translational dynamics near the membrane.[28,29] In addition, the flexibility of the membrane, associated with its bending elasticity, can also affect the dynamics of probes inside the capsule.

In this work, the tracking of the colloidal motion embedded in the inner cavity of 5–30 µm GUVs, obtained by electroformation,[30] has been studied in order to try to elucidate some of the most fundamental physical rules governing the dynamics of a simple model under well-defined conditions of restriction of the accessible volume. The proposed model allows the analysis of how the modification of the characteristic length of the confinement cage and/or the viscosity of the microenvironment within the inner cavity of the GUVs affect the motion of colloidal beads. This is possible by studying the quasi-2D motion of colloidal beads under two different experimental conditions: i) A single colloidal bead diffusing in the water confined within the inner cavity of GUVs of different diameter, and ii) a single colloidal bead diffusing in a viscous media formed for an aqueous solution of sodium alginate (concentration of 0.5 g L^{-1}) confined within the inner cavity of GUVs. GUVs of different diameters were used to simultaneously mimic the confinement and viscoelastic effects present in the cell cytoplasm.

2. Results

2.1. Particle Motion in the Inner Cavity of GUVs

The diffusive 2D motion of a single colloidal polystyrene sulfate latex bead of diameter $a = 1.6$ µm confined within the aqueous environment encapsulated for the lipid bilayers of GUVs was followed by videomicroscopy. **Figure 1** shows snapshots obtained for a diffusing colloidal bead (Figure 1A–D) imaged at different times during its diffusion within the internal cavity of a GUV. The motion can be described in terms of the 2D trajectory shown in Figure 1E as

$$\Delta y = y(t) - y(0) \tag{1}$$

versus

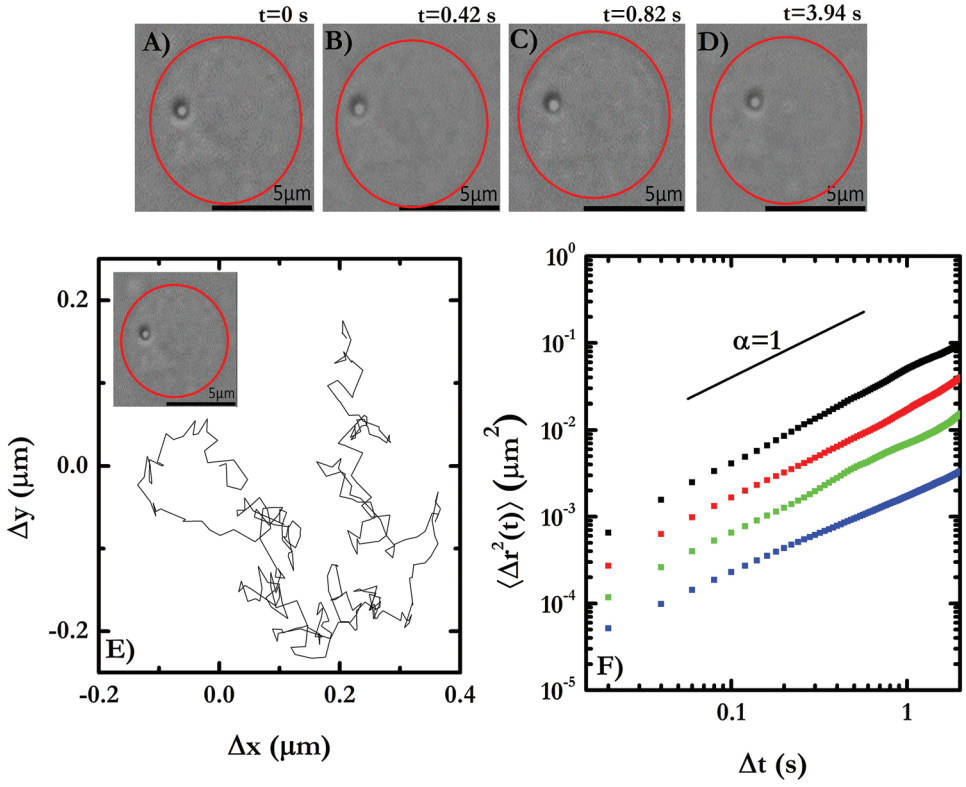

Figure 1. Results of single particle tracking experiments of colloidal beads confined in the aqueous interior of a GUV. A–D) Snapshots obtained for a colloidal bead imaged at different times during its diffusion within the inner cavity of a GUV. E) Typical trajectory projected onto the *x*–*y* plane for a colloidal bead ($a = 1.6$ µm) diffusing in the aqueous environment contained within a GUV. The inset shows the GUV of panels (A–D) with the position of its walls indicated by a red circle. F) MSD plotted against lag time on log–log scale for colloidal beads diffusing within the inner cavity of GUVs having different diameters (■ 7.1 µm, ■ 11.0 µm, ■ 22.0 µm and ■ 32.8 µm). A line corresponding to a value of $\alpha = 1$ is also included in the plot.

$$\Delta x = x(t) - x(0) \tag{2}$$

where $x(t)$ and $y(t)$ are the coordinates of the 2D motion of the bead at t time. In the particular case corresponding to the trajectory of a particle encapsulated in the aqueous inner core of a GUV, the motion cannot be properly described by a random walk as would be expected for a Brownian motion, suggesting that confinement can drive the emergence of an anomalous dynamics in the motion of colloidal microbeads.

The analysis of the trajectories makes it possible to calculate the mean-square displacement (MSD) for the 2D motion of a single bead

$$\left\langle \Delta r^2(t) \right\rangle = \left\langle \left| x(t) - x(0) \right|^2 + \left| y(t) - y(0) \right|^2 \right\rangle \tag{3}$$

where the brackets indicate the average between several trajectories (at least 20 independent trajectories were evaluated for each experiment).[31] Figure 1F shows the dependence of the MSD on the lag time (Δt) obtained from the analysis of the trajectories of the particle motion obtained by videomicroscopy (see Section 4 for details) for different cage dimensions, that is, GUVs of different diameters. The measured MSD describes a quasi-linear function on the lag time within the experimental window, independently of the dimensions of the GUVs. This dependence can be described in terms of the Einstein's diffusion power-law for a 2D motion ($\langle \Delta r^2(t) \rangle = 4D\Delta t^{\alpha}$, where D corresponds to the 2D translational diffusion coefficient and α is the anomalous diffusion exponent (see Section 4 for details).

The diffusion of a bead confined in the inner cavity of the GUVs is found to depend on the size of the confining cage L, that is, the diameter of the vesicle. For small values of L, the bead motion becomes superdiffusive, which is very different from the quasi-Brownian motion ($\alpha = 1.013 \pm 0.001$, and diffusion coefficient $D_0 = 0.059 \pm 0.002$ μm^2 s^{-1}) found for the diffusion of the unconfined colloidal bead within an aqueous environment. This is clearly observed in **Figure 2**A where the exponent α is plotted versus the normalized confinement area $\xi = (a/L)^2$. It should be noted that the higher the ξ value the smaller the area available for particle motion.

The results show that the encapsulation of particles in GUVs affects to the hydrodynamic conditions driving the particle motion, leading to anomalous diffusion. This appears to be strongly dependent on the size of the confining cage. Thus, at the highest values of the size of the confining cage (lower ξ values), subdiffusive motion was observed for the confined bead within the inner cavity of the GUVs.[32] However, the emergence of a superdiffusive regime under strong confinement conditions ($\xi > 0.02$), that is, at the highest values of ξ or for GUVs with the smallest diameter, seems to be a counterintuitive finding.

The increase in ξ forces to a motion of the bead close to the cage wall, that is, internal leaflet of the GUVs. This situation is very unstable according to the results by Aponte-Rivera and Zia,[33] who reported that the presence of the cavity wall enhances the diffusion of the particle, forcing its migration far from the cage boundaries. This explains the appearance of the superdiffusive regime under strong confinement conditions, because the approach of the bead to the walls introduces a repulsive force between the wall of the GUVs and the colloidal bead. This leads to an enhancement in the mobility of the particle, which results in superdiffusion. It can therefore be concluded that as the dimension of the confining cage is reduced, the passive motion of the colloidal bead starts to be hydrodynamically coupled to the action of the symmetric interaction potential emerging from the confining wall.

The different regimes of anomalous diffusion are also evidenced by the ξ dependence of the diffusion coefficient of the colloidal bead normalized to its value when diffusing following a Brownian pathway in an aqueous medium D_0 shown in Figure 2B. Regardless of the dimensions of the confining cage, a decrease in the apparent diffusion coefficient is observed with respect to that of freely diffusing beads. On the other hand, the reduction of the confinement, that is, the decrease of ξ, leads to a reduction of the diffusion coefficient down to a value about 2 orders of magnitude lower than the apparent diffusion coefficient of the free particle, remaining rather constant in the subdiffusive regime. However, the diffusion coefficient undergoes a strong increase within the superdiffusive regime,

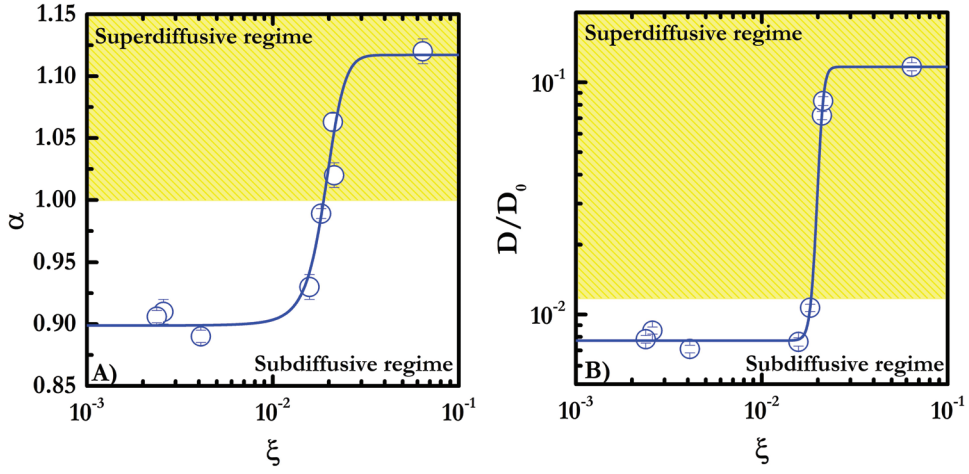

Figure 2. A) Anomalous diffusion exponent α and B) reduced diffusion coefficient D/D_0 as a function of the normalized confinement area $\xi = (a/L)^2$ for colloidal beads diffusing in GUVs of different diameters. The lines are guides for the eye.

although it remains below the D_0 value, independently of the confinement strength, as ξ increases above 0.02. This increase in the diffusion coefficient can be understood as a consequence of the enhanced mobility of the particles associated with the reduction of the available space. A similar behavior was predicted for the diffusion of active matter under parabolic confinement. Therefore, the results indicate that the passive dynamics of colloidal probes moving under a strong symmetric confinement (accessible volume is comparable to probe dimensions) is reminiscent of that expected for particles actuated with an external symmetric potential.[32]

2.2. Particle Motion under Confinement in a Viscoelastic Fluid: Toward an Understanding of the Colloidal Motion in the Cytoplasm

As mentioned above, confinement is not the only contribution that drives the anomalous diffusion within the cytoplasm.[34,35] In fact, the cytoplasm resembles a viscoelastic confined environment, where the accessible volume for the diffusion of molecules and macromolecules undergoes a stronger reduction than that expected by the confinement effect.[36] As a first step, this situation can be mimicked by replacing the water from the inner cavity of the GUVs by a viscoelastic solution.[37] In this work, GUVs filled with sodium alginate solutions (concentration 0.5 g L^{-1}) were used as model cells, in which the viscoelastic solution represents the internal cell core. Before analyzing the motion of the colloidal beads within a viscoelastic confined medium, it is interesting to analyze the colloidal diffusion in a simple viscoelastic sodium alginate solution. **Figure 3**A shows the dependence of the MSD on the lag time (Δt) obtained from the analysis of the trajectories of the particle motion within solutions of different concentrations of sodium alginate ($c_{\text{sodium alginate}}$). For the sake of comparison, the dependence corresponding to the Brownian diffusion in water is also shown.

Diffusion in a viscoelastic fluid, such as the sodium alginate solutions, slows down the motion of the colloidal bead compared to that in water. This is reflected in the decrease of the slope (below 1) of the curves shown Figure 3A. In fact, the α

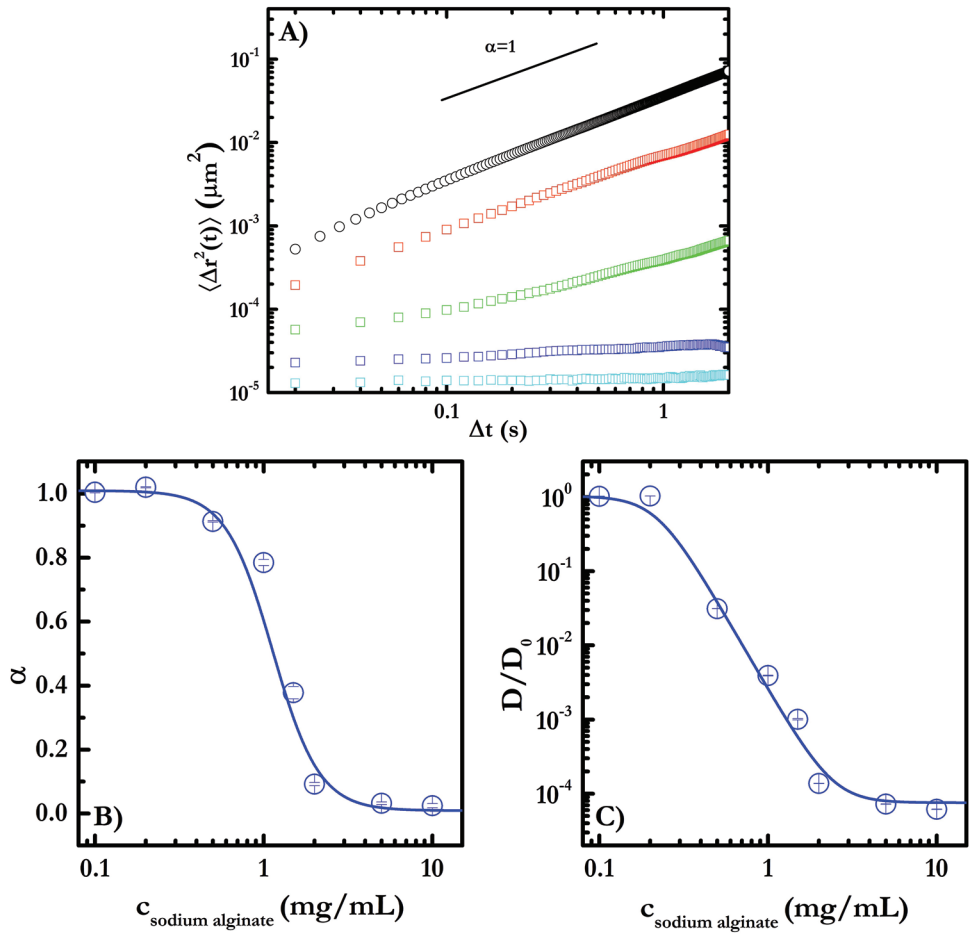

Figure 3. A) MSD plotted against lag time on a log–log scale for colloidal beads diffusing in water and in a sodium alginate solution of different concentrations as were obtained from single particle tracking experiments. ○ Diffusion in water. □ Diffusion in sodium alginate solution (0.5 g L^{-1}). □ Diffusion in sodium alginate solution (1 g L^{-1}). □ Diffusion in sodium alginate solution (2 g L^{-1}). □ Diffusion in sodium alginate solution (10 g L^{-1}). A line corresponding to a value of $\alpha = 1$ is also included in the plot. B) Anomalous diffusion exponent α as a function of the sodium alginate concentration for colloidal beads diffusing in aqueous solutions. C) Reduced diffusion coefficient D/D_0 as a function of the of the sodium alginate concentration for colloidal beads diffusing in aqueous solutions. The lines in panels (B) and (C) are guides for the eye.

exponent drops from a value close to the unity for solutions with the lowest sodium alginate concentration to quasi null values for the highest concentrated solutions (see Figure 3B), and thus the motion enters in a subdiffusion regime. This is due to the higher viscosity of sodium alginate solutions compared to water (almost one order of magnitude),[2,38] which introduces a viscous delay to the colloidal bead motion. In addition, the polymer chains may introduce a volume exclusion contribution to the free diffusion of the colloidal bead. Therefore, the colloidal bead may remain locally trapped, resulting in the slowing down of the dynamics.[39]

The influence of the viscoelastic nature of the sodium alginate solutions is also reflected in the value of the diffusion coefficient. This decreases by a factor of 10^4 with respect to that corresponding to the diffusion of the colloidal bead in water with the increase of the solution concentration up to 10 g L^{-1} b (see Figure 3C), which is qualitatively reasonable according to the Stokes-Einstein equation. Thus, it is expected that the increase in the viscosity of the medium will reduce the diffusivity of the colloidal bead. This must be considered as a result of the increase in the contribution of the viscous drag force opposing to the particle motion, in agreement with the predictions of the Enskog theory. This predicts a decrease in the diffusion coefficient of a hard sphere as the steric hindrance to its motion increases with the increase in the volume fraction of molecules in the medium.[40] Moreover, considering that $D_0/D_{\text{sodium alginate}} \neq \eta_{\text{sodium alginate}}/\eta_0$ (for sodium alginate solutions of 5 and 10 g L^{-1}, the ratio of the diffusion coefficients assumes a value of about 10^4,[38] whereas that of the viscosities assumes values about 8 and 11, respectively), where D_0 and $D_{\text{sodium alginate}}$ are the diffusion coefficients of the colloidal bead within water and sodium alginate solutions, respectively, and η_0 and $\eta_{\text{sodium alginate}}$ are the viscosities of water and sodium alginate solutions, respectively. The results indicate that the slowing down of the effective diffusivity in the viscoelastic medium is a result of the combined action of the viscous drag force and the excluded volume effects.

Table 1. Values of the diffusion coefficient and α exponent corresponding to the motion of the colloidal bead in water and sodium alginate aqueous solution (0.5 g L^{-1}).

Medium	D [$\mu m^2\ s^{-1}$]	α
Water	$(5.9 \pm 0.2)\times10^{-2}$	1.013 ± 0.001
Sodium alginate (0.5 g L^{-1})	$(1.840 \pm 0.001)\times10^{-3}$	0.913 ± 0.002

For the sake of comparison, **Table 1** summarizes the values of the diffusion coefficient and the α exponent corresponding to the unconfined motion of the colloidal bead in water and in aqueous sodium alginate solution at a concentration of 0.5 g L^{-1}, which is the same as that used for the studies in confined media.

On the basis of the above results, and taking into account the individual effects of the confinement and the viscoelasticity of the medium on the colloidal particle motion, it can be expected that the situation can become even more complex when both conditions are present simultaneously.[41] **Figure 4**A shows the dependence of the α exponent on ξ for the diffusion of colloidal particles in a sodium alginate solution caged in GUVs of different diameters. Again, the results show that increasing ξ leads to an increase in α. However, for particles diffusing in an environment combining both viscoelasticity and confinement, the values of α always remain below those obtained for the diffusion in a medium where only confinement is considered (see inset in Figure 4A). Furthermore, the combination of viscoelasticity and confinement leads the particle motion to a subdiffusive dynamics, regardless of the dimension of the caging GUVs.

It is clear that the results show a counteracting role of viscoelasticity and confinement. Thus, increasing the viscosity of the medium reduces the importance of the repulsive force associated with colloidal motion in the vicinity of the walls. This leads to a situation where the combination of the dissipation of translational energy resulting from the excluded volume effects and the hydrodynamic interactions pushes the colloidal

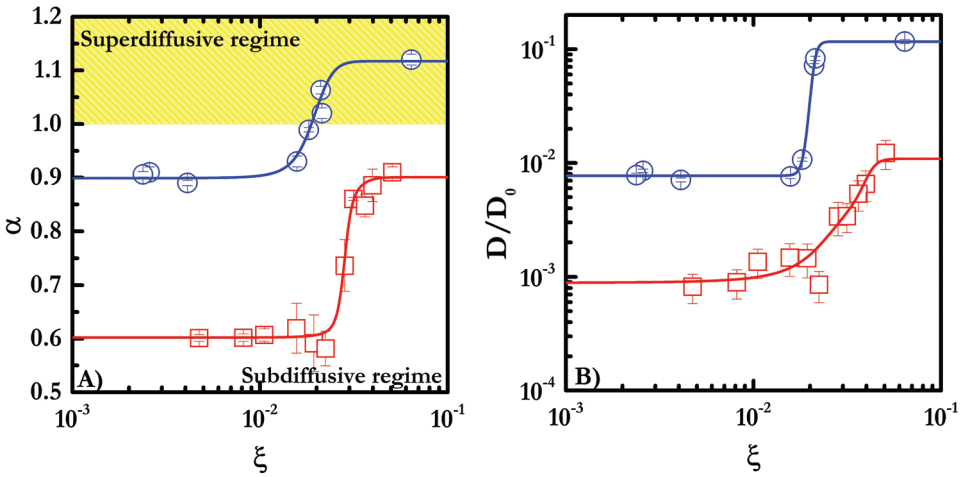

Figure 4. A) Anomalous diffusion exponent α and B) reduced diffusion coefficient D/D_0 as a function of the normalized confinement area $\xi = (a/L)^2$ for colloidal beads diffusing within GUVs of different diameters. ○ Diffusion in GUVs filled with water and □ diffusion in GUVs filled with sodium alginate solution. The lines are guides for the eye.

motion into a subdiffusive regime. This is consistent with the results by Roosen-Runge et al.[42] for protein diffusion in non-Newtonian fluids such as those considered here. Therefore, the enhancement of motion associated with the strongest confinement conditions is counteracted by the increase of the viscosity of the fluid environment. On the other hand, the subdiffusive character of the motion found at the weakest confinement conditions is strongly enhanced by the viscoelastic nature of the medium. It should be stressed that the colloidal motion under strong confinement conditions, when the medium is viscoelastic, has a similar subdiffusive character to the diffusion of the bead in an unconfined viscoelastic medium. This can only be understood by considering that the viscoelasticity of the medium allows to overcome the enhanced diffusivity induced by the presence of the confinement boundary. In the light of the results, it is possible to suggest the existence of a characteristic value of ξ (around 3×10^{-2}) which represents a crossover point between two regimes on the dynamics of the colloidal bead under symmetric confinement conditions. The first regime, which occurs at the lowest values of ξ is characterized by a motion controlled by the specific conditions of the environment, including the combination of confinement and the specific viscoelasticity of the medium, whereas the second regime, which occurs at the highest values of ξ, is mainly governed by the restriction of the available volume due to the confinement, independently of the nature of the medium.

The analysis of the changes of in the diffusion coefficient (see Figure 4B) as a result of the introduction of viscoelasticity into the colloidal motion under confinement conditions shows the slowing down of the diffusion rate.[43] However, this hydrodynamic constraint is not sufficient to justify the reduction of the diffusion coefficient by more than one order of magnitude with respect to the system where only confinement is considered. This can therefore be taken as confirmation that both the viscous drag force and the interactions between the particles and the polymer chains play a very important role. Furthermore, the results for viscoelastic alginate solutions show that under strong confinement conditions, there is a significant reduction in the diffusion coefficient of the confined bead compared to that of the unconfined one, while the anomalous exponent α remains almost unchanged in agreement with the findings by Harusawa et al.[44]

3. Conclusion

GUVs offer an excellent environment for study the diffusion of colloidal beads under controlled conditions of confinement viscoelasticity. In this work, the effect of the dimension of the confinement cage, L, and the presence of a viscoelastic fluid in the inner cavity of the GUVs, on the motion of colloidal beads of a fixed diameter ($a = 1.6$ μm) are investigated. Both the confinement and the viscoelasticity force the anomalous diffusion of the colloidal beads, but their effects are counteracting. This can be understood by considering the different hydrodynamic boundary conditions introduced by confinement and viscoelasticity. On the other hand, both confinement and viscoelasticity decrease the diffusion coefficient with respect to the dilute limit (Brownian diffusion in water), which can be understood considering the role of the hydrodynamic interactions. However, when viscoelasticity and confinement act simultaneously, the hydrodynamic interactions associated with the viscous drag are not enough to explain the slowing of diffusion, and the exclude volume interactions between the particles and the polymer chains play a non-negligible role on the slowing of diffusion.

It is expected that this work can serve as a tool for the systematic elucidation of the key parameter governing the motion of molecular and supramolecular objects in complex confined and viscoelastic environments, for example, the cell cytoplasm. Furthermore, the identification and characterization of colloidal motion mechanisms can contribute to the understanding of mass transport phenomena occurring in complex systems, thus contributing to different scientific and technological problems, including separation techniques, drug encapsulation and delivery, transport in cells, microfluidic systems, or the fabrication of hierarchical nanomaterials.

4. Experimental Section

Materials: Soybean L-α-phosphatidylcholine (PC) with a purity ≥ 99%, supplied by Acros Organics (Geel, Belgium), was used for the preparation of the lipid vesicles. Chloroform (CHROMASOLV, for High Performance Liquid Chromatography, stabilized with ethanol) and with indium tin oxide (ITO)-coated glass slides were purchased from Sigma-Aldrich (Saint Louis, MO, USA). Polystyrene sulfate latex beads with diameter of 1.6 μm and polydispersity index of 0.08 were purchased as an aqueous dispersion with a concentration of 8% w/v from Invitrogen Corp. (Carlsbad, CA, USA). D(+)-sucrose (analytical grade, purity > 99.5%, hereafter sucrose), D(+)-glucose (analytical grade, purity > 99.5%, hereafter glucose), and sodium alginate were purchased from Sigma-Aldrich (Saint Louis, MO, USA).

Ultrapure deionized water used for cleaning and preparation of the dispersions was obtained using a multicartridge purification system AquaMAX-Ultra 370 Series. (Young Lin Instrument Co., Ltd., Gyeonggi-do, South Korea), presenting a resistivity higher than 18 MΩ·cm, and a total organic content lower than 6 ppm (Milli-Q quality).

Lipid Film Preparation: Lipid thin films were prepared on ITO-coated glass slides. For this purpose, a lipid solution with a concentration of 1 g L^{-1} is deposited by dropping onto the surface of an ITO-coated glass slide. Then, the solvent was evaporated by placing the slip in an oven at 50 °C for a period of 1 h.

Preparation of GUVs by Electroformation: The formation of GUVs by electroformation relied on the modulation of the swelling of the lipid film deposited on the ITO-coated glass slide in an aqueous environment (sucrose solution with a concentration of 0.3 M) using an externally applied electric field. This required the use of an electroformation chamber formed by two parallel ITO-coated glass coverslips separated by a Viton o-ring and connected to the electrical circuit by two pieces of conductive copper tape (RS Components, Corby, UK). Once the chamber was filled and sealed, an AC electric field was applied using a function generator (Agilent 33120A, Agilent Technologies, Inc., Santa Clara, CA, USA), which enabled the control of the frequency (f) and amplitude (V_{pp}) of the applied electric field. The preparation of GUVs filled with colloidal beads was carried out by including the beads as a suspension during the hydration process. This allowed to obtain GUVs with colloidal beads remaining trapped within their aqueous inner cavity.

GUVs were formed following a single step electroformation procedure based on the application of an electrical field with a constant value of the frequency and voltage to the electroformation chamber for a fixed time of 1 h.[30,45,46] In order to obtain GUVs with different diameters, the frequency and voltage of the applied electric field were varied in the range 10^1–10^4 Hz and 2–10 V, respectively. The formation of GUVs in such frequency and voltage ranged may be related to the existence of an optimal

electro-osmotic flow for the hydration and swelling of the initial lipid film,[47] and therefore the absence of GUV formation when an electric films with low voltage and high frequency is applied can be explained in terms of the weakness and high velocity of the electro-osmotic vibrations, which limit the swelling process of the film.[48] Furthermore, increasing the voltage for a fixed value of frequency also reduced the possibility of formation of GUVs, which can be rationalized by considering that although at such high voltage the mechanical agitation was high enough to ensure the detachment of the lipid film, the amplitude of the electro-osmotic oscillation at a fixed frequency decreased with the voltage of the electric field. Therefore, the mechanical agitation was not enough to facilitate the bilayer separation and the formation of the GUVs.[48–50]

Imaging: Optical microscopy images of microbead diffusion were obtained using a Nikon Eclipse 80i microscope equipped with a 50 × 0.55 NA objective (model LU Plan, Nikon, Japan) and coupled to a ORCA-Flash4.0 V3 CMOS camera (model C13440-20CU, Hamamatsu Photonics K.K., Japan) camera. For single particle tracking, images of 2048 × 2048 pixels^2 corresponding to 130 × 130 μm^2 were obtained at 30 fps. It should be noted that the visualization of samples containing GUVs required the dispersion of the initial suspension of electroformed vesicles in an aqueous glucose solution (concentration 0.3 M). This dilution provided enough refractive index difference between the internal region of the GUVs (aqueous solution containing mainly sucrose) and the external one (aqueous solution containing mainly glucose) to allow the determination of the position of the external bilayer of the GUVs. The observation chamber was formed by a microscope slide (Rogo-Sampaic, Wissous, France) and a microscope cover slip (Menzel-Glaser, Braunschweig, Germany) joined by double-sided adhesive tape. The sample was introduced by capillarity into the chamber, which was then sealed with silicone oil with a viscosity of about 200 mPa (Sigma-Aldrich, Saint Louis, MO, USA).

Single Particle Tracking: The coordinates of the diffusing beads were obtained from time series of 2D images using a custom-written particle tracking software (Particle Tracker v. 2.4.0.5).[51–53] This software allows one to obtain the trajectories of the beads by a frame-by-frame analysis of the recorded sequences using a routine based on the centroiding technique,[54] which provides the exact *x*- and *y*- positions of a particle at a time *t*. Thus, it is possible to compute the MSD for the quasi-2D motion (MSD, $\langle r^2 \rangle$). The MSD as function of the lag time Δt can be described by a power-law $\langle r^2 \rangle \propto t^{\alpha}$, where α defines the anomalous diffusion exponent. For a system with normal Brownian diffussion, $\alpha = 1$, whereas anomalous diffusion is characterized by $\alpha \neq 1$ ($0 < \alpha <$ 1 corresponds to subdiffusion, $\alpha > 1$ to superdiffusion and $\alpha = 2$ to a ballistic diffusion).[55,56] Error analysis was performed by averaging the trajectories obtained in 25 videos obtained under the same conditions and calculating the standard error.

Acknowledgements

This work was partly funded by MINECO (Spain) under grant PID2019-106557GB-C21, and by the E.U. in the framework of the European Innovative Training Network-Marie Sklodowska-Curie Action NanoPaInt (grant agreement 955612). The help of Andrea Ramayo and Ana María García Mora González with some preliminary experiments is acknowledged.

Conflict of Interest

The authors declare no conflict of interest.

Data Availability Statement

The data that support the findings of this study are available on request from the corresponding author. The data are not publicly available due to privacy or ethical restrictions.

Keywords

anomalous diffusion, colloidal particles, confinement, diffusion, giant unilamellar vesicles, hydrodynamics, viscoelastic medium

Received: March 12, 2023
Revised: April 13, 2023
Published online: April 28, 2023

[1] H. X. Zhou, G. Rivas, A. P. Minton, *Annu. Rev. Biophys.* **2008**, *37*, 375.
[2] G. A. Siddiqui, A. Naeem, *J. Mol. Liquids* **2021**, *322*, 114602.
[3] D. Gnutt, M. Gao, O. Brylski, M. Heyden, S. Ebbinghaus, *Angew. Chem., Int. Ed.* **2015**, *54*, 2548.
[4] S. B. Zimmerman, S. O. Trach, *J. Mol. Biology* **1991**, *222*, 599.
[5] R. J. Ellis, A. P. Minton, *Nature* **2003**, *425*, 27.
[6] T. Sentjabrskaja, E. Zaccarelli, C. De Michele, F. Sciortino, P. Tartaglia, T. Voigtmann, S. U. Egelhaaf, M. Laurati, *Nat. Commun.* **2016**, *7*, 11133.
[7] D. Orsi, T. Rimoldi, E. Guzmán, L. Liggieri, F. Ravera, B. Ruta, L. Cristofolini, *Langmuir* **2016**, *32*, 4868.
[8] D. Orsi, E. Guzmán, L. Liggieri, F. Ravera, B. Ruta, Y. Chushkin, T. Rimoldi, L. Cristofolini, *Sci. Rep.* **2015**, *5*, 17930.
[9] S. K. Ghosh, A. G. Cherstvy, D. S. Grebenkov, R. Metzler, *New J. Phys.* **2016**, *18*, 013027.
[10] B. Wang, S. M. Anthony, S. C. Bae, S. Granick, *Proc. Natl. Acad. Sci. U. S. A.* **2009**, *106*, 15160.
[11] S. B. Zimmerman, A. P. Minton, *Annu. Rev. Biophys. Biomol. Struct.* **1993**, *22*, 27.
[12] C. Echeverria, R. Kapral, *J. Chem. Phys.* **2010**, *132*, 104902.
[13] A. Dhar, A. Samiotakis, S. Ebbinghaus, L. Nienhaus, D. Homouz, M. Gruebele, M. S. Cheung, *Proc. Natl. Acad. Sci. U. S. A.* **2010**, *107*, 17586.
[14] D. M. Hatters, A. P. Minton, G. J. Howlett, *J. Biol. Chem.* **2002**, *277*, 7824.
[15] R. Chapanian, D. H. Kwan, I. Constantinescu, F. A. Shaikh, N. A. A. Rossi, S. G. Withers, J. N. Kizhakkedathu, *Nat. Commun.* **2014**, *5*, 4683.
[16] A. Soranno, I. Koenig, M. B. Borgia, H. Hofmann, F. Zosel, D. Nettels, B. Schuler, *Proc. Natl. Acad. Sci. U. S. A.* **2014**, *111*, 4874.
[17] M. Sarkar, A. E. Smith, G. J. Pielak, *Proc. Natl. Acad. Sci. U. S. A.* **2013**, *110*, 19342.
[18] H. Al-Obaidi, A. T. Florence, *J. Drug Delivery Sci. Technol.* **2015**, *30*, 266.
[19] B. R. Parry, I. V. Surovtsev, M. T. Cabeen, C. S. O'Hern, E. R. Dufresne, C. Jacobs-Wagner, *Cell* **2014**, *156*, 183.
[20] T. Cherdhirankorn, V. Harmandaris, A. Juhari, P. Voudouris, G. Fytas, K. Kremer, K. Koynov, *Macromolecules* **2009**, *42*, 4858.
[21] J. Choi, M. J. A. Hore, N. Clarke, K. I. Winey, R. J. Composto, *Macromolecules* **2014**, *47*, 2404.
[22] S. Salami, C. Rondeau-Mouro, J. van Duynhoven, F. Mariette, *J. Agric. Food Chem.* **2013**, *61*, 5870.
[23] S. Park, I. Park, T. Chang, C. Y. Ryu, *J. Am. Chem. Soc.* **2004**, *126*, 8906.
[24] C. C. Striemer, T. R. Gaborski, J. L. McGrath, P. M. Fauchet, *Nature* **2007**, *445*, 749.
[25] J. van den Berg, A. J. Boersma, B. Poolman, *Nat. Rev. Microbiol.* **2017**, *15*, 309.
[26] M. Tsugane, H. Suzuki, *ACS Synth. Biol.* **2020**, *9*, 2819.
[27] H. Jia, P. Schwille, *Curr. Opin. Biotechnol.* **2019**, *60*, 179.
[28] H. Terasawa, K. Nishimura, H. Suzuki, T. Matsuura, T. Yomo, *Proc. Natl. Acad. Sci. U. S. A.* **2012**, *109*, 5942.
[29] W.-C. Su, D. L. Gettel, M. Chabanon, P. Rangamani, A. N. Parikh, *J. Am. Chem. Soc.* **2018**, *140*, 691.

[30] H. Bi, B. Yang, L. Wang, W. Cao, X. Han, *J. Mater. Chem. A* **2013**, *1*, 7125.
[31] P. G. Saffman, M. Delbrück, *Proc. Natl. Acad. Sci. U. S. A.* **1975**, *72*, 3111.
[32] H. E. Ribeiro, F. Q. Potiguar, *Phys. A* **2016**, *462*, 1294.
[33] C. Aponte-Rivera, R. N. Zia, *Phys. Rev. Fluids* **2016**, *1*, 023301.
[34] G. Guigas, M. Weiss, *Biophys. J.* **2008**, *94*, 90.
[35] B. M. Regner, D. Vučinić, C. Domnisoru, T. M. Bartol, M. W. Hetzer, D. M. Tartakovsky, T. J. Sejnowski, *Biophys. J.* **2013**, *104*, 1652.
[36] J.-F. Berret, *Nat. Commun.* **2016**, *7*, 10134.
[37] J. Ma, Y. Lin, X. Chen, B. Zhao, J. Zhang, *Food Hydrocolloids* **2014**, *38*, 119.
[38] M. A. Masuelli, C. O. Illanes, *Int. J. BioMat. Sci. Eng.* **2014**, *1*, 1.
[39] R. Sahoo, L. Theeyancheri, R. Chakrabarti, *Soft Matter* **2022**, *18*, 1310.
[40] K. Miyazaki, *J. Chem. Phys.* **2001**, *114*, 6276.
[41] J. T. Mika, B. Poolman, *Curr. Opin. Biotechnol.* **2011**, *22*, 117.
[42] F. Roosen-Runge, M. Hennig, F. Zhang, R. M. J. Jacobs, M. Sztucki, H. Schober, T. Seydel, F. Schreiber, *Proc. Natl. Acad. Sci. U. S. A.* **2011**, *108*, 11815.
[43] G. Nawrocki, P.-H. Wang, I. Yu, Y. Sugita, M. Feig, *J. Phys. Chem. B* **2017**, *121*, 11072.
[44] K. Harusawa, C. Watanabe, Y. Kobori, K. Tomita, A. Kitamura, M. Kinjo, M. Yanagisawa, *Langmuir* **2021**, *37*, 437.
[45] Q. Wang, X. Zhang, T. Fan, Z. Yang, X. Chen, Z. Wang, J. Xu, Y. Li, N. Hu, J. Yang, *Micromachines* **2017**, *8*, 24.
[46] S. E. Ghellab, W. Mu, Q. Li, X. Han, *Biophys. Chem.* **2019**, *253*, 106217.
[47] D. S. Dimitrov, M. I. Angelova, *Prog. Colloid Polym. Sci.* **1987**, *73*, 48.
[48] H. Morgan, N. Green, *AC Electrokinetics: Colloids And Nanoparticles*, Research Studies Press, Ltd., Hertfordshire, UK **2003**.
[49] R. Dimova, S. Aranda, N. Bezlyepkina, V. Nikolov, K. A. Riske, R. Lipowsky, *J. Phys.: Condens. Matter* **2006**, *18*, S1151.
[50] T. J. Politano, V. E. Froude, B. Jing, Y. Zhu, *Colloids Surf., B* **2010**, *79*, 75.
[51] A. Maestro, L. J. Bonales, H. Ritacco, T. M. Fischer, R. G. Rubio, F. Ortega, *Soft Matter* **2011**, *7*, 7761.
[52] L. J. Bonales, J. E. F. Rubio, H. Ritacco, C. Vega, R. G. Rubio, F. Ortega, *Langmuir* **2011**, *27*, 3391.
[53] L. J. Bonales, F. Martínez-Pedrero, M. A. Rubio, R. G. Rubio, F. Ortega, *Langmuir* **2012**, *28*, 16555.
[54] J. C. Crocker, D. G. Grier, *J. Colloid Interface Sci.* **1996**, *179*, 298.
[55] Y. Chen, X. Wang, W. Deng, *Phys. Rev. E: Stat., Nonlinear, Biol., Soft Matter Phys.* **2019**, *99*, 042125.
[56] R. Metzler, J. Klafter, *Phys. Rep.* **2000**, *339*, 1.